



## True near field versus contrast near field imaging. II. imaging with a probe

Jean-Baptiste Masson, Guilhem Gallot

### ► To cite this version:

Jean-Baptiste Masson, Guilhem Gallot. True near field versus contrast near field imaging. II. imaging with a probe. Optics Express, 2007, 15 (6), pp.3078. 10.1364/OE.15.003078 . hal-00824235

HAL Id: hal-00824235

<https://polytechnique.hal.science/hal-00824235>

Submitted on 1 Oct 2013

**HAL** is a multi-disciplinary open access archive for the deposit and dissemination of scientific research documents, whether they are published or not. The documents may come from teaching and research institutions in France or abroad, or from public or private research centers.

L'archive ouverte pluridisciplinaire **HAL**, est destinée au dépôt et à la diffusion de documents scientifiques de niveau recherche, publiés ou non, émanant des établissements d'enseignement et de recherche français ou étrangers, des laboratoires publics ou privés.

# True near field versus contrast near field imaging. II. imaging with a probe

Jean-Baptiste Masson and Guilhem Gallot

Laboratoire d'Optique et Biosciences, Ecole Polytechnique, CNRS, INSERM,

91128 Palaiseau, France

[jean-baptiste.masson@polytechnique.edu](mailto:jean-baptiste.masson@polytechnique.edu)

[guilhem.gallot@polytechnique.edu](mailto:guilhem.gallot@polytechnique.edu)

**Abstract:** In this letter, we extend the results previously found in near field imaging with aperture [Opt. Express 14, 11566 (2006)], where we demonstrated that interaction between light and sample can be divided into two main areas: the true near field and the contrast near field domain. Here, we show that in near field with a probe, the same division of space exists, and thus we show that a much simpler way to model these experiments can be given.

© 2007 Optical Society of America

**OCIS codes:** (110.0180) Microscopy; (260.0260) Diffraction Theory

---

## References and links

1. J.-B. masson and G. Gallot, "True near field versus contrast near field imaging," Opt. Express **14**, 11566-11574 (2006).
2. A. Lewis, H. Taha, A. Strinkovski, A. Manevitch, A. Khatchatourians, R. Dekhter, and E. Ammann, "Near-field optics: from subwavelength illumination to nanometric shadowing," Nature biotechnol. **21**, 1378-1386 (2003).
3. Y. Lu, T. Wei, F. Duewer, Y. Lu, N.-B. Ming, P. G. Schultz, and X.-D. Xiang, "Nondestructive imaging of dielectric-constant profiles and ferroelectric domains with a scanning-tip microwave near-field microscope," Science **276**, 2004-2006 (1997).
4. D. Molenda, G. C. d. Francs, U. C. Fischer, N. Rau, and A. Naber, "High-resolution mapping of the optical near-field components at a triangular nano-aperture," Opt. Express **13**, 10688-10696 (2005).
5. J. P. Fillard, *Near Field Optics and Nanoscopy*, (World Scientific, Singapore, 1996).
6. Comsol. Burlington, MA, USA, Version 3.3.
7. M. A. Bhatti, *Fundamental Finite Element Analysis and Applications: With Mathematica and Matlab Computations*, (J. Wiley & Sons, Hoboken, New Jersey, 2005).
8. J.-B. Masson, M.-P. Sauviat, J.-L. Martin, and G. Gallot, "Ionic contrast terahertz near field imaging of axonal water fluxes," Proc. Nat. Acad. Sci. USA **103**, 4808-4812 (2006).
9. J.-B. masson, M.-P. Sauviat, and G. Gallot, "Ionic contrast terahertz time resolved imaging of frog auricular heart muscle electrical activity," Appl. Phys. Lett. **89**, 153904 (2006).
10. M. Born and E. Wolf, *Principles of optics 6th Edition*. (Cambridge University Press, Cambridge, 1997).
11. A. Bouhelier, M. Beversluis, A. Hartschuh, and L. Novotny, "Near-field second-harmonic generation induced by local field enhancement," Phys. Rev. Lett. **90**, 013903 (2003).
12. H. Cory, A. C. Boccara, J. C. Rivoal, and A. Lahrech, "Electric field intensity variation in the vicinity of a perfectly conducting conical probe: Application to near-field microscopy," Microwave Opt. Technol. Lett. **18**, 120-124 (1998).

---

## 1. Introduction

Near field optics has the very interesting possibility of breaking through the limit of diffraction, and offers the ability to image with a precision much better than the wavelength of the electromagnetic radiation used [2, 3, 4, 5]. A sample smaller than the incident electromagnetic

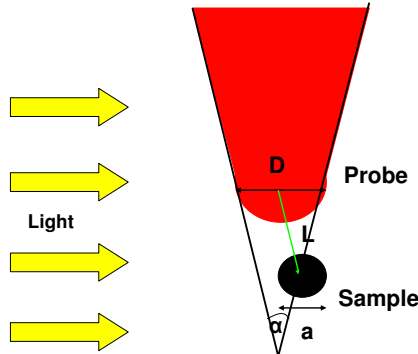


Fig. 1. Principle of apertureless near field microscopy. The probe has a cone angle  $\alpha$ . The sample is a sphere of diameter  $a$ , at a distance  $L$  from the center of the probe apex of diameter  $D$ .

wavelength re-emits light with a spatial frequency directly related to its size. However, this information is absent from the wave propagating in the far field, and near field measurements are required to image with subwavelength precision. Typically, an aperture with sub-wavelength diameter is positioned and moved very close to the sample under study. We recently demonstrated that the treatment of this interaction could be strongly simplified. We showed the existence of two specific domains in near field imaging: True Near Field (TNF) and Contrast Near Field (CNF) domains [1]. In TNF domain, mutual interaction between the object and the aperture leads to very complex analysis. On the contrary, in CNF domain, near field interactions still allow sub-wavelength measurements, but the sample weakly perturbs the aperture field distribution. Therefore, simple Green function propagation treatment is allowed.

However, further improvements are mainly limited by the transmission through the aperture, which decreases as the third power of the diameter. An alternative widely used is apertureless near field microscopy, where the aperture is replaced by a conic probe. Here, the probe tip is put close to the sample in order to locally modify the electric constant. Once again, mutual interactions between probe and sample are the source of the complexity of the near field analysis and a reason why finite element programming [6, 7] is almost always used to precisely analyze the results. The question of defining a CNF domain for this system is however more complex, since the conic probe breaks the symmetry of the system, and since the whole probe diffracts the light over a large distance. Here, we demonstrate again the existence of a division of near field interaction space between TNF and CNF domains. We show that analysis in CNF is possible in apertureless near field imaging, and can be divided in two steps: first, a full 3D finite element analysis of the probe, and second, a simple field propagation using Green functions.

## 2. Simulation model and results

The system is depicted in Fig. 1 and is studied using two different procedures. The first is the complete solving of the full system, sample and probe, by full 3D *ab initio* finite element method programming [7, 8, 9]. It is the direct local resolution of the Maxwell's equations. This procedure can be found in Ref. [1]. The second procedure requires several steps. First, Maxwell's equations are solved in the system containing the probe alone, with 3D finite element method. Then, the electric field around the probe is extracted from the calculation and Green function propagation method is employed [1]. Classic scalar Green functions [10] are used to transfer the electric field from both the source and the probe around the sample to the far

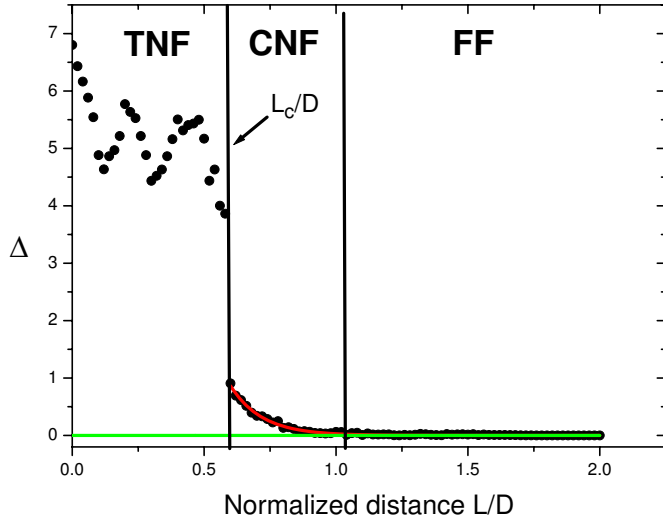


Fig. 2. Example, for a spherical sample of normalized size 0.22, of the evolution of  $\Delta$  with normalized distance  $L/D$ . Three domains have been pointed out: the TNF, CNF and far field domains. The red line is the exponential fit in the CNF domain. The green line is far field reference.

field detection domain. The propagated field is the convolution between the Green functions, describing the sample and the propagation media, and the calculated field around the probe. The convolution is performed at the point where the field is detected.

Most characteristics of the calculation are similar to the one used for near field imaging with aperture [1]. In near field with aperture, a great care was payed to the mesh inside the aperture. This issue is even more difficult here. The main difference between the two calculations is the locking of the mesh near the probe. Between different simulations, noticeable changes in the mesh structure near the probe can be noticed. Nevertheless, these changes do not lead to detectable modifications of electric field values near the probe, and so do not alter the results of the calculations. The size of the simulation boxes in the probe calculation is chosen to be much larger than the one used in the aperture calculation, in order to take into account the length of the probe, and to avoid the proximity between the probe and the limits of the simulation box. Thus, the simulation boxes were separated to the probe and the sample by at least  $3\lambda$ .

In analyzing near field imaging with aperture, two parameters were defined to characterize the interactions between the sample and the aperture. The first one was related to direct experimental research, *i.e.* energy detection.  $\Delta$  was the difference between the energy calculated by 3D finite element method and Green function propagation at the detection point in the far field domain. The second one was linked to the very structure of near field interaction and was the maximal electric field gradient  $\nabla_M$  between the probe and the sample. The latter was very useful, since it was less sensitive to geometry variation of both the aperture and the sample. Here, as the geometric effect of the probe is irrelevant,  $\nabla_M$  is much less clearly defined in apertureless near field experiments. Therefore, the  $\Delta$  parameter is sufficient to describe most of experiments and is only discussed here. On Fig. 2, we show an example of the evolution of  $\Delta$  with the normalized distance between the sample and the probe. Very interestingly, the behavior of  $\Delta$  in apertureless near field interaction is very similar to the one with aperture. It is not an obvious result, since in near field with aperture [1], the light that interacts with the sample has only been

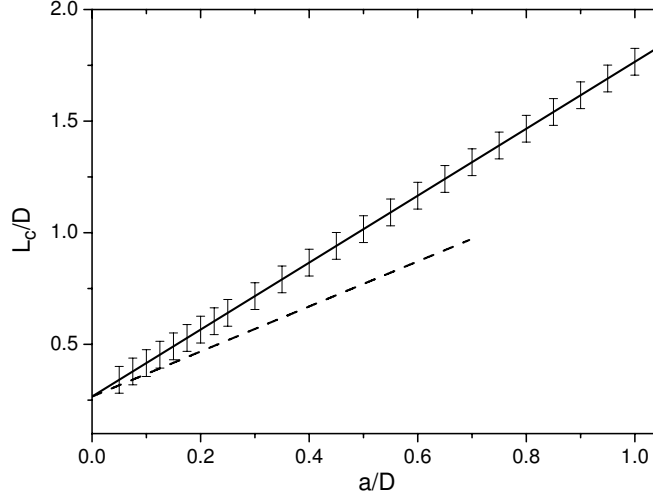


Fig. 3. Evolution of the normalized distance  $L_c/D$  versus  $a/D$ . The solid line corresponds to the linear fit of the simulations, and the error bars refer to the dispersion of the results for  $D/\lambda$  from  $1/3$  to  $1/9$ . The dotted line refers to near field with aperture.

scattered by the aperture. In apertureless near field, the light interacts at the same time with both the probe and the sample.

Three domains are observable. First, a domain where  $\Delta$  is almost null. This domain corresponds to the far field domain. As the distance decreases,  $\Delta$  differs from its far field value. Its evolution is, at first, monotone. The limit of this domain is the distance  $L_c$  (where  $\Delta$  can no longer be approximated 0). The behavior of  $\Delta$  is no longer monotone when  $L < L_c$  and corresponds to a third domain, characterized by a more complex behavior. The apparent discontinuity between the two domains is clearly due to the numerical simulations and is not physical. In all simulations similar behaviors for both parameters have been encountered. The limit of the two near field domains are investigated, so the evolution of  $L_c$  versus  $a/D$  and  $D/\lambda$  (Fig. 3) and the evolution of  $\Delta$  versus the normalized shifted distance  $d = (L - L_c)/D$  (Fig. 4) are studied. First, it should be noticed that  $L_c$  and  $\Delta$  are independent of the probe tip normalized size. From Fig. 3,  $L_c$  evolves as a linear function of the normalized size of the sample. We may notice that the slope of the linear fit is larger than the one found with near field in aperture (1.5 for probe and 1 for aperture). It characterizes the fact that the TNF domain is wider in apertureless near field than in near field with aperture. The main difference between the probe and the aperture is the potential influence of the cone of the probe. Several studies [11, 12] investigated the influence of the cone and showed that the cone acts as an antenna concentrating the electromagnetic field on the tip. Another parameter has then been investigated: the apex angle  $\alpha$  of the probe (see Fig. 1). Results are shown in Fig. 5. There seems to be no real influence of the angle on the limit between the CNF and TNF domain. However, this does not mean that the angle has no influence at all on the near field interactions. This angle plays a role on the intensity of the resulting field at the tip [12], as well as on the contrast of the imaging [5]. The geometry of the probe has an impact on the contrast of the higher order diffracted electric field, *i.e.* higher order of interaction.

Furthermore, in the CNF domain ( $L > L_c$ ),  $\Delta$  can be approximate as  $\Delta \propto e^{-\frac{d}{D/8}}$  (Fig. 4), a decreasing exponential function of  $d$ , with a characteristic distance  $D/8$ . In the CNF domain of imaging with aperture, the characteristic decreasing distance was found to be only  $D/10$ .

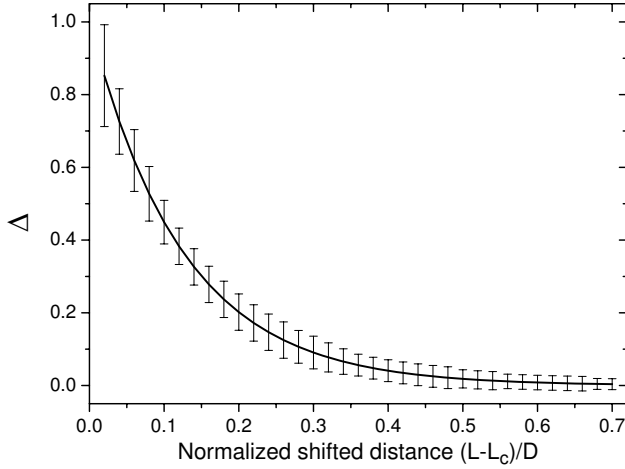


Fig. 4. Exponential fit (solid line) of the overall evolution  $\Delta$  with the normalized displacement distance  $(L - L_c)/D$ , for 3 tip sizes:  $\lambda/2$ ,  $\lambda/5$  and  $\lambda/10$ . The error bars show the dispersion of the results for each tip size and for 8 values of  $a/D$  from 0.05 to 0.75. The characteristic distance of the exponential is  $D/8$ .

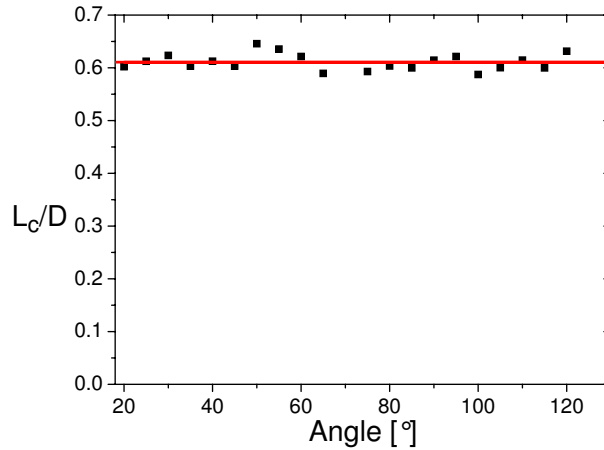


Fig. 5. Evolution of the normalized distance  $L_c/D$  with the main angle of the probe. This example is taken with  $a/D=0.22$ . Black points are the results and the red line is the mean value found in the linear model of the evolution of  $L_c/D$  with  $a/D$ .

This is the main difference between the two systems. In near field imaging with aperture, light sequentially interacts with the aperture and then with the sample. Here, light almost simultaneously interacts with both the probe and the sample. Mutual interaction is therefore stronger, due to higher order interactions between the radiated dipoles of the probe in the near field domain. Furthermore, here again the influence of the cone angle of the probe is negligible and there is no modification of the characteristic decreasing distance with  $\alpha$ . Finally, it should be noticed that the behavior of  $\Delta$  is independent of the normalized size of the sample.

Results on the evolution of  $\Delta$  and  $L_c$  confirm the existence, in apertureless near imaging, as

well as with aperture, of an interesting spatial domain, the CNF domain, in which the spatial resolution of near field still exists, and in which simple calculation may be achieved. From the limit of far field domain to the distance  $L_c$ , is the CNF interaction domain. There,  $\Delta$  may be approximated to 0. In this domain the sample "feels" the near field effect of the probe, but modifies only slightly the electric field around it. So a separate evaluation of the fields around the probe and around the sample can be performed. When the probe is closer to the sample, calculations become much more complex and require a full 3D simulation. It should be noted that, on the contrary to the theory developed for near field with aperture, a good parameter describing, in a very general way, the electric field inside the TNF domain is lacking. Nevertheless, the study performed on aperture near field tends to indicate that a suitable parameter should describe some topology changes in the electric field. Any attempt to describe pure intensity, would encounter major difficulties because of the very high sensitivity of the field in this domain.

Finally we may comment the difference between near field with aperture, and apertureless near field. Results show first, that evolution of  $L_c/D$  for the probe exhibits a higher slope than for the aperture and second, that the characteristic distance of the decreasing exponential describing the evolution of  $\Delta$  is inferior for the probe than for the aperture. Thus, in apertureless near field, the TNF domain and the CNF domain are wider than in near field with aperture, and in the CNF domain the decrease of  $\Delta$  is slower in apertureless near field than in near field with aperture. These results may be explained with the simplest model usually used to describe near field interaction: the dipole model [5]. In Near field with aperture, the light that interacts with the aperture, generates an induced dipole. This dipole emits an electromagnetic field which induces a dipole on the sample. TNF is then located in the domain where the interaction of the induced dipole of the sample interacts with the induced dipole of the aperture. In apertureless near field, the same light both induces a dipole on the probe and on the sample. Thus, we may understand the differences between the two kinds of near field, to be a difference of induced dipole order of interaction.

During the first phases of near field imaging development, it was easier to design probes than apertures, so apertureless near field became popular. Nevertheless, today, both kinds of near field are more easily handled with new technologies of probe and aperture design. From the results of this study, we may prefer near field with aperture, because it leads to an easier access to CNF, and provides an easier analysis of near field experiment, especially when the sample is much smaller than the aperture.

### 3. Conclusion

In this paper, we have extended the work performed on near field with aperture to apertureless near field imaging. Results demonstrated that in apertureless near field interaction, two domains can also be considered: the true near field domain and the contrast near field domain. In the true near field domain, interactions between sample and probe are strong and complex, and so the electric field in the domain between these is profoundly modified. In contrast near field domain, the probe still interacts with the sample, but the electric field near the probe is not strongly perturbed by the sample. In this domain  $\Delta$  is monotonous and exhibit a decreasing exponential behavior of characteristic distance  $D/8$ . The limit  $L_c$  between the two domains is linearly dependent of the size of the sample.

In TNF experimental conditions analyzing results implies a complete resolution of Maxwell's equation with full 3D finite element method simulations. In CNF experimental conditions,  $\Delta$  may be approximated to 0, and the analysis is divided in two steps, a 3D finite element method analysis and Green function propagation. This analysis method is much simpler and faster, and the small loss of spatial precision is compensated by the precise physical information gathered

from it.